# Hydron Transfer Catalyzed by Triosephosphate Isomerase. Products of Isomerization of Dihydroxyacetone Phosphate in $D_2O$[†]

AnnMarie C. O'Donoghue, Tina L. Amyes, and John P. Richard*

*Department of Chemistry, University at Buffalo, SUNY, Buffalo, New York 14260-3000*

*Received September 22, 2004; Revised Manuscript Received December 1, 2004*

ABSTRACT: The product distributions for the reactions of dihydroxyacetone phosphate (DHAP) in $D_2O$ at pD 7.9 catalyzed by triosephosphate isomerase (TIM) from chicken and rabbit muscle were determined by $^1$H NMR spectroscopy using glyceraldehyde 3-phosphate dehydrogenase to trap the first-formed products of the thermodynamically unfavorable isomerization reaction, (*R*)-glyceraldehyde 3-phosphate (GAP) and [2(*R*)-$^2$H]-GAP (*d*-GAP). Three products were observed from the reactions catalyzed by TIM: GAP from isomerization with intramolecular transfer of hydrogen (18% of the enzymatic products), *d*-GAP from isomerization with incorporation of deuterium from $D_2O$ into C-2 of GAP (43% of the enzymatic products), and [1(*R*)-$^2$H]-DHAP (*d*-DHAP) from incorporation of deuterium from $D_2O$ into C-1 of DHAP (40% of the enzymatic products). The ratios of the yields of the deuterium-labeled products *d*-DHAP and *d*-GAP from partitioning of the intermediate of the TIM-catalyzed reactions of GAP and DHAP in $D_2O$ are 1.48 and 0.93, respectively. This provides evidence that the reaction of these two substrates does not proceed through a single, common, reaction intermediate but, rather, through distinct intermediates that differ in the bonding and arrangement of catalytic residues at the enediolate O-1 and O-2 oxyanions formed on deprotonation of GAP and DHAP, respectively.

We are interested in characterizing and understanding the dynamics of hydron transfer during the reversible 1,2-hydrogen shift catalyzed by triosephosphate isomerase (TIM), which results in the interconversion of dihydroxyacetone phosphate (DHAP)[1] and (*R*)-glyceraldehyde 3-phosphate (GAP, Scheme 1) (*1*). TIM catalyzes the reversible stereospecific deprotonation of its substrates DHAP and GAP to form an enzyme-bound enediol(ate) intermediate (*2, 3*). Proton transfer from substrate to Glu-165 at TIM "labels" the protein with an isotope of hydrogen that may be different from the isotope of hydrogen present in the bulk solvent. For example, when the substrate and solvent water are essentially 100% enriched in $^1$H (hydrogen) and $^2$H (deuterium), respectively, the TIM−enediol(ate) complex labeled at Glu-165 with $^1$H derived from substrate may undergo intramolecular transfer of $^1$H to form product labeled with $^1$H. Alternatively, it can undergo effectively irreversible hydron exchange with bulk solvent (*2, 3*), resulting in formation of the deuterium-labeled triose phosphates [1(*R*)-$^2$H]-DHAP (*d*-DHAP*)* and [2(*R*)-$^2$H]-GAP (*d*-GAP).

Scheme 1

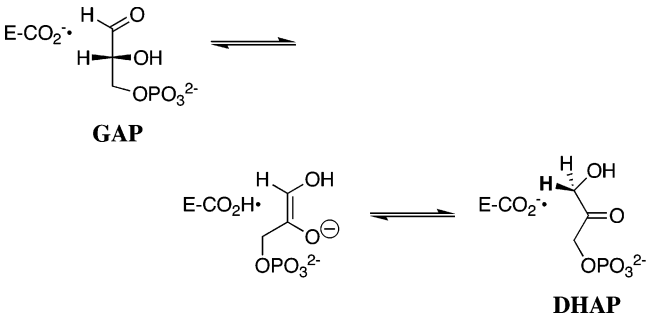


Two ratios of macroscopic rate constants may be calculated from the yields of the products of the TIM-catalyzed reaction of $^1$H-labeled substrate in $D_2O$. (1) The rate constant ratio for partitioning of the $^1$H-labeled TIM−enediol(ate) intermediate between intramolecular hydrogen transfer and hydron exchange with solvent $D_2O$, $(k_{C\text{-}1})_H/k_{ex}$ or $(k_{C\text{-}2})_H/k_{ex}$ (parts A and B of Scheme 2, respectively), may be calculated as the ratio of the yields of the hydrogen and deuterium-labeled products of the TIM-catalyzed reactions of GAP and DHAP, respectively. (2) The rate constant ratio for partitioning of the $^2$H-labeled TIM−enediol(ate) intermediate between deuterium transfer to C-1 and C-2 may be calculated as the ratio of the yields of *d*-DHAP and *d*-GAP from the reactions of both GAP and DHAP.

$^1$H NMR spectroscopy is a powerful analytical method that can be used to monitor the deprotonation of carbon acids, because this leads to the incorporation of deuterium from

[†] This work was supported by Grant GM 39754 from the National Institutes of Health. J.P.R. thanks the Science Foundation of Ireland for a Walton Fellowship, during which time this manuscript was prepared.

* To whom correspondence should be addressed. Tel: (716) 645 6800, ext 2194. Fax: (716) 645 6963. E-mail: jrichard@chem.buffalo.edu.

[1] Abbreviations: TIM, triosephosphate isomerase; GPDH, glyceraldehyde 3-phosphate dehydrogenase; LDH, L-lactic dehydrogenase; DHAP, dihydroxyacetone phosphate; GAP, (*R*)-glyceraldehyde 3-phosphate; *d*-DHAP, [1(*R*)-$^2$H]-dihydroxyacetone phosphate; *d*-GAP, [2(*R*)-$^2$H]-glyceraldehyde 3-phosphate; D,L-GAP, D,L-glyceraldehyde 3-phosphate; *h*-PGA, (*R*)-3-phosphoglycerate; *d*-PGA, [2(*R*)-$^2$H]-3-phosphoglycerate; NAD, nicotinamide adenine dinucleotide, oxidized form; NADH, nicotinamide adenine dinucleotide, reduced form; EDTA, ethylenediamine tetraacetic acid; NMR, nuclear magnetic resonance.

10.1021/bi047953k CCC: $30.25 
Published on Web 01/28/2005

Scheme 2


solvent $D_2O$ into the carbon acid (*4*−*13*). In the preceding paper we reported that the TIM-catalyzed reaction of GAP in $D_2O$ results in 49%, 31%, and 21% yields of DHAP, *d*-DHAP, and *d*-GAP, respectively (*1*). This requires similar rate constants for partitioning of the $^1$H-labeled TIM−enediol(ate) intermediate between intramolecular hydrogen transfer to form DHAP and hydron exchange with solvent $D_2O$ to form *d*-DHAP and *d*-GAP, so that $(k_{C\text{-}1})_H \approx k_{ex}$ (Scheme 2A). This 49% *intramolecular* transfer of hydrogen is much larger than the up to 6% *intramolecular* transfer of tritium label from substrate to product GAP observed for the TIM-catalyzed isomerization of [1(*R*)-$^3$H]-DHAP in $H_2O$ (*14*−*16*). Our observation that a large fraction of the TIM-catalyzed reaction of GAP in $D_2O$ proceeds with intramolecular hydrogen transfer shows there is only limited equilibration of the catalytic base labeled with the substrate-derived hydrogen at the TIM−enediol(ate) complex with the hydrons of bulk solvent.

The experiments described in this paper were designed to determine the product distribution for the thermodynamically unfavorable TIM-catalyzed isomerization of DHAP in $D_2O$ (Scheme 2B) and were initiated for two reasons.

(1) The observation that the reaction of GAP catalyzed by TIM in $D_2O$ proceeds with extensive (49%) intramolecular transfer of hydrogen from substrate to product was unexpected, because of the previous reports that only low levels of intramolecular transfer of tritium are observed for the TIM-catalyzed reaction of [1(*R*)-$^3$H]-DHAP in $H_2O$ (*14*−*16*). The apparent discrepancy in these observations might be due to the fact that these experiments monitor the isomerization reaction in different directions. Alternatively, it may be related to the use of different solvents and combinations of hydrogen isotopes. We therefore wanted to determine the yields of the products of the TIM-catalyzed isomerization of DHAP in $D_2O$, to compare the extent of this reaction that proceeds with intramolecular transfer of hydrogen with the extent of the TIM-catalyzed isomerization of [1(*R*)-$^3$H]-DHAP in $H_2O$ that proceeds with intramolecular transfer of tritium (*14*−*16*).

(2) The nonenzymatic base-catalyzed deprotonation of GAP and DHAP in water leads to two different enediolate oxyanions which differ in the position of the negative charge at O-1 and O-2, respectively, and which equilibrate faster than their reprotonation at carbon (*17*). Similarly, the TIM-catalyzed deprotonation of GAP and DHAP also gives different intermediates at which negative charge at the two enediolate oxygens is stabilized by interaction with the neutral imidazole side chain of His-95 (*18*−*20*). However, it is not clear whether the equilibration of these intermediates, which requires the movement of both a proton and an amino acid side chain(s) within the restricted confines of an enzyme active site, is fast relative to their turnover to product. If there is rapid equilibration of these distinct intermediates, then the TIM-catalyzed reactions of GAP and DHAP in $D_2O$ should result in formation of the deuterium-labeled products *d*-DHAP and *d*-GAP *in the same ratio*. However, if the equilibration of these different intermediates is slow relative to their reprotonation at carbon, then the ratio of the yields of *d*-DHAP and *d*-GAP from partitioning of the intermediates generated in the TIM-catalyzed reactions of GAP and DHAP may be different.

## MATERIALS AND METHODS

Except as detailed below, all materials and methods were described in the previous paper (*1*). L-Lactic dehydrogenase from rabbit muscle (970 units/mg) and glyceraldehyde 3-phosphate dehydrogenase from baker's yeast (72 units/mg) were purchased from Sigma. Sodium hydrogenarsenate heptahydrate, EDTA (disodium salt), and pyruvic acid (sodium salt) were purchased from Aldrich. NAD and (*R*)-3-phosphoglyceric acid (disodium salt) were purchased from Sigma.

Chloroacetol 3-phosphate diethyl ketal (biscyclohexylammonium salt) was a generous gift from Professor Albert Mildvan. Hydrolysis of the ketal at room temperature in 0.13 M DCl in $D_2O$ was monitored by $^1$H NMR spectroscopy until it was ca. 99% complete. The resulting solution of chloroacetol 3-phosphate was then adjusted to pD ~2 with NaOD and stored at −20 °C. Immediately before use, an aliquot of this stock solution was adjusted to pD 6 by the addition of 1 M $NaHCO_3$. The very small amounts of TIM present in our solutions of commercial yeast glyceraldehyde 3-phosphate dehydrogenase (250 $\mu$M) and rabbit muscle L-lactic dehydrogenase (250 $\mu$M) were inactivated by incubation with 27 $\mu$M chloroacetol phosphate for 10 min at 4 °C (*16*). These enzymes were then freed of the inactivator by passage over a column of Sephadex G-25 equilibrated with 100 mM triethanolamine-HCl buffer (pH 7.6) containing 5 mM EDTA.

*Enzyme Assays.* All enzyme assays were carried out at 25 °C. L-Lactic dehydrogenase was assayed at pH 7.5 (100 mM imidazole) by monitoring the enzyme-catalyzed oxidation of NADH (0.1 mM) by pyruvate (1.3 mM) at 340 nm. Glyceraldehyde 3-phosphate dehydrogenase was assayed at pH 7.5 (75 mM imidazole) by monitoring the enzyme-catalyzed reduction of NAD (0.03 mM) by GAP (1.7 mM, added as 3.4 mM D,L-GAP) in the presence of sodium hydrogenarsenate (30 mM) at 340 nm.

TIM was assayed by coupling the isomerization of DHAP to the reduction of NAD using glyceraldehyde 3-phosphate dehydrogenase (*21*), monitored at 340 nm. The assay mixture contained 80 mM imidazole (pH 7.5, $I = 0.1$, NaCl), 0.1 mM NAD, 15 mM sodium hydrogenarsenate, 5 mM DHAP, and 0.6 units of glyceraldehyde 3-phosphate dehydrogenase in a volume of 1 mL at $I = 0.15$ (NaCl). The concentration of DHAP in these assays and in the turnover of DHAP by TIM in $D_2O$ monitored by $^1$H NMR was obtained from the

change in absorbance at 340 nm upon its complete reduction by NADH catalyzed by glycerol 3-phosphate dehydrogenase.

*$^1$H NMR Analyses.* The following $^1$H NMR spectral data were obtained for authentic 3-phosphoglyceric acid in $D_2O$ buffered with 80 mM imidazole at pD 7.9 and $I = 0.15$ (NaCl): $\delta$ 4.07 ppm (1H, m, $J_{AB} = 5.9$ Hz, $J_{AC} = 2.8$ Hz, $J_{HP} \approx 0.9$ Hz, $CH_AOD$); 3.91 ppm (1H, m, $J_{AB} = 5.9$ Hz, $J_{BC} = 10.9$ Hz, $J_{HP} = 6$ Hz, $CH_BH_COPO_3^{2-}$); 3.77 ppm (1H, m, $J_{AC} = 2.8$ Hz, $J_{BC} = 10.9$ Hz, $J_{HP} = 6$ Hz, $CH_BH_COPO_3^{2-}$). Relaxation times $T_1 = 2-4$ s were determined for these protons.

*TIM-Catalyzed Isomerization of DHAP in $D_2O$ Monitored by $^1$H NMR.* The turnover of DHAP (5 mM) by rabbit or chicken muscle TIM in the presence of 80 mM imidazole buffer (pD 7.9), 15 mM sodium hydrogenarsenate, 7 mM sodium pyruvate, 0.1 mM NAD, glyceraldehyde 3-phosphate dehydrogenase (0.3−0.6 units/mL) and L-lactic dehydrogenase (1.3−1.5 units/mL) in $D_2O$ at 25 °C and $I = 0.15$ (NaCl) was followed by $^1$H NMR spectroscopy. For experiments with chicken muscle TIM the reaction mixture also contained 2 mM tetramethylammonium hydrogensulfate as an internal standard.

Identical 800 $\mu$L aliquots of the reaction mixture without TIM were placed in two separate NMR tubes. In one tube the enzyme-catalyzed reaction was initiated by the addition of 10 $\mu$L of TIM in buffered $D_2O$ and the tube was incubated at 25 °C. Meanwhile, the $^1$H NMR spectrum of the reaction mixture in the absence of TIM was recorded using the aliquot in the other tube. The progress of the reaction of DHAP in both the presence and absence of TIM was then monitored by $^1$H NMR spectroscopy at 25 °C. The absorbance at 340 nm was monitored in a separate control solution that was identical with those used for the $^1$H NMR experiments, except that it contained a larger quantity (0.056 unit/mL) of TIM.

The observed peak areas $A_{obs}$ for the reactant DHAP and the products *d*-DHAP, (*R*)-3-phosphoglycerate (*h*-PGA), [2(*R*)-$^2$H]-3-phosphoglycerate (*d*-PGA), and methylglyoxal determined by integration of $^1$H NMR spectra obtained at various reaction times were normalized according to eq 1.

$$A_P = A_{obs}\left(\frac{(A_{std})_0}{A_{std}}\right) \quad (1)$$

$$A_H = (A_{DHAP})_0/2 \quad (2)$$

$$f_{DHAP} = \frac{A_{DHAP}/2}{A_H} \quad (3)$$

$$f_{d-DHAP} = \frac{A_{d-DHAP}}{A_H} \quad (4)$$

$$f_{h-PGA} = \frac{A_{h-PGA}}{A_H} \quad (5)$$

$$f_{d-PGA} = \frac{A_{d-PGA}}{A_H} \quad (6)$$

$$f_{MG} = \frac{\{A_{MG} - (A_{MG})_0\}/0.60}{A_H} \quad (7)$$

The disappearance of DHAP was followed by monitoring the decrease in the sum of the normalized areas $A_{DHAP}$ of the singlets at 3.44 and 4.44 ppm due to the two protons of the $CH_2OD$ groups of the hydrate and keto forms of DHAP, respectively, calculated using eq 1. The fraction of DHAP remaining at time *t* was calculated using eq 3, where $A_H$ is the normalized peak area for a *single* proton of *total* DHAP at $t = 0$, calculated using eq 2.

The formation of *d*-DHAP was followed by monitoring the appearance of the broad singlet at 3.42 ppm and the triplet ($J_{HD} = 2-3$ Hz) at 4.42 ppm due to the single proton of the CHDOD groups of the hydrate and keto forms of *d*-DHAP, respectively. The fraction of DHAP converted to *d*-DHAP was calculated from the *sum* of the normalized peak areas of the signals due to a single proton of the hydrate and keto forms of this product according to eq 4.

The formation of *h*-PGA was followed by monitoring the appearance of the signal due to its C-2 proton at 4.07 ppm, and the fraction of DHAP converted to *h*-PGA was calculated using eq 5. It was not possible to resolve $^1$H NMR signals that are unique to the product *d*-PGA. However, the *combined* yield of *h*-PGA and *d*-PGA is proportional to half the observed area of all the signals due to the C-3 protons of both these compounds, $A_{C-3H}/2$, while the yield of *h*-PGA alone is proportional to the area of the signal due to its C-2 proton, $A_{h-PGA}$. Therefore, the peak area due to a *single* C-3 proton of *d*-PGA was calculated using the relationship $A_{d-PGA} = (A_{C-3H}/2) - A_{h-PGA}$.

The formation of methylglyoxal was followed by monitoring the singlet at 5.17 ppm due to the C-1 proton of the monohydrate (*1*). The fraction of DHAP converted to methylglyoxal was calculated from the *increase* in the normalized area of this singlet, $A_{MG} - (A_{MG})_0$, using eq 7, where 0.60 is the fraction of methylglyoxal present as the C-1 monohydrate (*1*).

## RESULTS

The TIM-catalyzed reaction of dihydroxyacetone phosphate (5 mM) in $D_2O$ in the presence of 80 mM imidazole buffer (pD 7.9) at 25 °C and $I = 0.15$ (NaCl) was monitored by $^1$H NMR spectroscopy. In these experiments the thermodynamically unfavorable ($K_{eq} = 1/22$) (*22*) isomerization of DHAP to (*R*)-glyceraldehyde 3-phosphate (GAP) and [2(*R*)-$^2$H]-glyceraldehyde 3-phosphate (*d*-GAP) was made effectively irreversible by using NAD to oxidize these products to give (*R*)-3-phosphoglycerate (*h*-PGA) and [2(*R*)-$^2$H]-3-phosphoglycerate (*d*-PGA) in reactions catalyzed by glyceraldehyde 3-phosphate dehydrogenase (GPDH, Scheme 3) (*21*). In preliminary experiments we found that the signals due to the protons of NAD and NADH overlapped with those due to the protons of the substrate DHAP and the reaction

Scheme 3

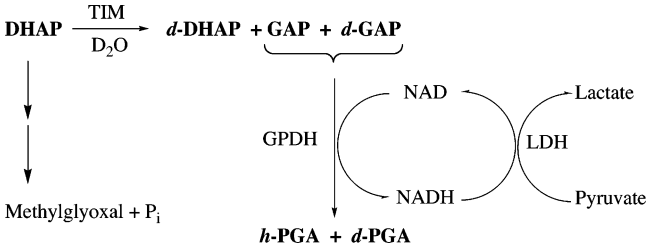


products. Therefore, the initial concentration of NAD (0.1 mM) was kept at only ca. 2% that of the initial concentration DHAP, and the oxidized form of the cofactor was rapidly regenerated by the reoxidation of NADH by pyruvate in a reaction catalyzed by L-lactic dehydrogenase (LDH, Scheme 3).

The absorbance at 340 nm due to NADH ($A_{340}$) was monitored in a reaction mixture that was comparable to those used to monitor the TIM-catalyzed turnover of DHAP in $D_2O$ by $^1H$ NMR spectroscopy, except that the concentration of TIM was ca. 10-fold greater than that used in the $^1H$ NMR experiments. Initiation of the reaction by the addition of TIM resulted in a rapid 0.03 unit increase in $A_{340}$, corresponding to the reduction of ca. 5% of the NAD to give NADH, followed by a slow return to the baseline absorbance over the next several hours. This shows that ca. 95% of the cofactor remains in the oxidized NAD form during the course of the TIM-catalyzed isomerization of DHAP in $D_2O$ monitored by $^1H$ NMR. Therefore, the inclusion of pyruvate and LDH in the reaction mixture resulted in effective "recycling" of the NAD cofactor (Scheme 3).

Several commercial preparations of GPDH were examined for use as a coupling enzyme for the rapid oxidation of GAP in these experiments. We had intended to use GPDH from rabbit or chicken muscle, because we reasoned that the presence of small amounts of contaminating muscle TIMs in these preparations should not affect the product distributions that we observe from the turnover of DHAP catalyzed by the "authentic" muscle isomerases. However, $^1H$ NMR analysis of control experiments in which DHAP was incubated with commercial GPDH from rabbit or chicken muscle (0.3−0.6 units/mL) in $D_2O$ showed that these preparations catalyze the rapid incorporation of deuterium from solvent into C-1 of DHAP. This exchange reaction is much faster than that expected for the low levels of TIM present as a contaminant and is very likely due to the presence of a contaminating Schiff base aldolase (*23*). In a further control experiment we showed that the commercial preparation of GPDH from baker's yeast catalyzed slow isomerization and deuterium exchange reactions of DHAP, but at nearly the same *relative* rates as does authentic rabbit or chicken muscle TIM. This is consistent with the presence of a low level of TIM present as a contaminant in this preparation of GPDH, and in one experiment this contaminating TIM was inactivated by pretreatment with chloroacetol phosphate (*16, 24*). Similar control experiments with the commercial LDH from rabbit muscle showed that this preparation contained a very low level of TIM, and this activity was removed in one experiment by pretreatment with chloroacetol phosphate.

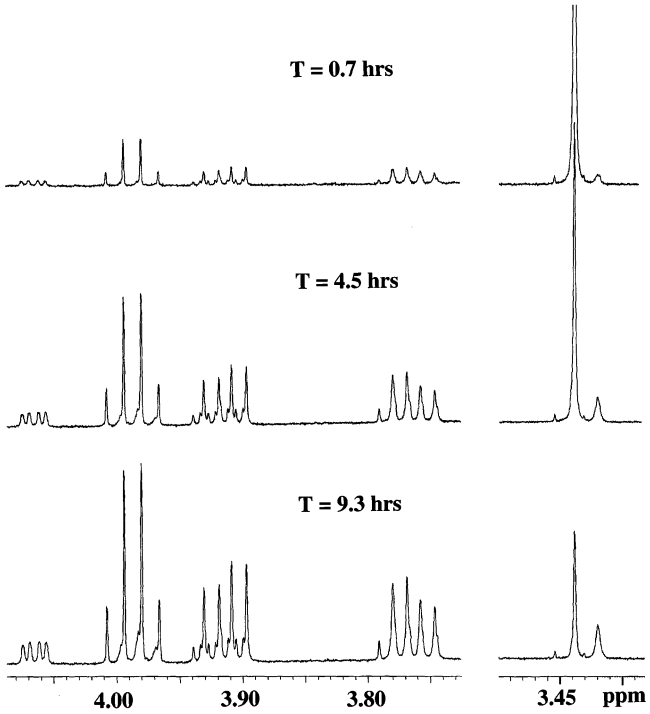


FIGURE 1: Representative partial $^1H$ NMR spectra of the remaining substrate and the products during the reaction of DHAP (5 mM) catalyzed by rabbit muscle TIM (0.0059 unit/mL) in $D_2O$ buffered by 80 mM imidazole at pD 7.9 and 25 °C ($I$ = 0.15, NaCl). The thermodynamically unfavorable isomerization of DHAP was coupled to oxidation of the first-formed products GAP and *d*-GAP to give *h*-PGA and *d*-PGA, respectively, using GPDH. The oxidized form of the NAD cofactor (0.1 mM) was regenerated by the oxidation of NADH by pyruvate catalyzed by LDH. The disappearance of the singlet at 3.44 ppm due to the $CH_2OD$ group of DHAP hydrate is accompanied by the appearance of a singlet at 3.42 ppm due to the CHDOD group of *d*-DHAP hydrate, a multiplet at 4.07 ppm due to the C-2 proton of *h*-PGA, and multiplets at 3.89−3.94 ppm and 3.74−3.79 ppm due to the diastereomeric C-3 protons of *both* *h*-PGA and *d*-PGA.

Figure 1 shows representative partial $^1H$ NMR spectra of the remaining substrate and the products during the reaction of DHAP (5 mM) catalyzed by chicken muscle TIM in $D_2O$ buffered by 80 mM imidazole at pD 7.9 and 25 °C ($I$ = 0.15, NaCl). In these experiments the first-formed isomerization products GAP and *d*-GAP were rapidly converted to *h*-PGA and *d*-PGA, respectively, by the action of baker's yeast GPDH, 15 mM sodium hydrogenarsenate, and 0.1 mM NAD. Rabbit muscle LDH and 7 mM pyruvate were also included in the reaction mixture, to ensure the regeneration of the NAD cofactor (Scheme 3). These $^1H$ NMR spectra show the following.

(1) The disappearance of the substrate DHAP with time, followed by monitoring the decrease in the singlet at 3.44 ppm due to the $CH_2OD$ group of DHAP hydrate and the singlet at 4.44 ppm due to the $CH_2OD$ group of the free keto form of DHAP (not shown) (*1*). The quartet at 3.99 ppm is due to the C-2 proton of L-lactate, formed by the LDH-catalyzed reduction of pyruvate by NADH (Scheme 3).

(2) The formation of the product [1(*R*)-$^2H$]-DHAP (*d*-DHAP) with time, followed by monitoring the appearance of the broad singlet (unresolved triplet) at 3.42 ppm due to the CHDOD group of *d*-DHAP hydrate and the triplet ($J_{HD}$ = 2−3 Hz) at 4.42 ppm due to the CHDOD group of the

free keto form of *d*-DHAP (not shown). These signals are shifted upfield by 0.019 and 0.025 ppm, respectively, from the corresponding signals for the $CH_2OD$ groups of DHAP hydrate and free DHAP (*1*).

(3) The formation of the products [2(*R*)-$^1$H]-3-phosphoglycerate (*h*-PGA) and [2(*R*)-$^2$H]-3-phosphoglycerate (*d*-PGA) from oxidation of the initial isomerization products GAP and *d*-GAP catalyzed by GPDH. The formation of *h*-PGA was followed by monitoring the appearance of the signal at 4.07 ppm due to its C-2 proton. The complex signals at 3.89−3.94 and 3.74−3.79 ppm are due to the diastereomeric C-3 protons of *both* *h*-PGA and *d*-PGA. The ratio of the areas of the signal at 4.07 ppm due to the C-2 proton of *h*-PGA and of either of the multiplets due to a *single* C-3 proton is only 0.3, which shows that *d*-GAP rather than *h*-GAP is the major product of the isomerization of DHAP catalyzed by TIM in $D_2O$. The area of the signals due to the C-3 protons is proportional to the *sum* of the yields of *h*-PGA and *d*-PGA, while the area of the signal at 4.07 ppm due to the C-2 proton is proportional to the yield of *h*-PGA alone. Therefore, the yield of *d*-PGA was calculated from the difference in the areas of the signals due to the C-3 and C-2 protons (see Materials and Methods).

(4) There is no detectable formation of GAP or *d*-GAP in these experiments, which shows that there is efficient trapping of these products by their irreversible oxidation to give *h*-PGA and *d*-PGA, respectively, catalyzed by GPDH. The upper limit on the amount of GAP or *d*-GAP that might have escaped detection in these experiments is 0.5% of the starting DHAP.

The formation of methylglyoxal in the competing nonenzymatic elimination reaction of DHAP (*17*) was followed by monitoring the singlet at 5.17 ppm due to the C-1 proton of methylglyoxal monohydrate. Methylglyoxal is the only significant product of the nonenzymatic reaction of DHAP because, in the presence of low concentrations of buffer at neutral pH, the enediolate phosphate formed by deprotonation of DHAP or GAP undergoes elimination of phosphate ca. 100-fold faster than protonation at carbon (*17*).

The fraction of substrate DHAP remaining (eq 3) and the fractional formation of the products (eqs 4−7) of the TIM-catalyzed and spontaneous reactions of DHAP at various reaction times were determined from the ratio of the normalized integrated peak area of the relevant signals due to the reactant or product (eq 1) and of the signal due to a *single* proton of *total* DHAP at $t = 0$ (eq 2), as described in Materials and Methods. The sum of the observed fractions of DHAP, *d*-DHAP, *h*-PGA, *d*-PGA, and methylglyoxal decreased by less than 10% during the reaction of up to 80% of the starting DHAP, which shows that all of the significant reaction products were identified by $^1$H NMR.

Figure 2A shows the decrease with time in the fraction of remaining DHAP during the reaction of DHAP (5 mM) catalyzed by chicken muscle TIM in $D_2O$ buffered by 80 mM imidazole at pD 7.9 and 25 °C ($I = 0.15$, NaCl), in the presence of 15 mM sodium hydrogenarsenate, 7 mM pyruvate, 0.1 mM NAD, GPDH (0.3 units/mL), and LDH (1.5 units/mL). Figure 2B shows the change in the fractional yields of the products that arise from the enzymatic reaction of DHAP in this experiment, $(f_P)_E$, which were normalized

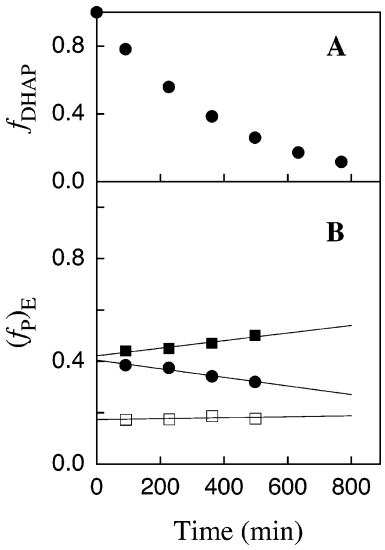


FIGURE 2: Product data for the reaction of DHAP (5 mM) catalyzed by chicken muscle TIM (0.0059 unit/mL) in $D_2O$ buffered by 80 mM imidazole at pD 7.9 and 25 °C ($I = 0.15$, NaCl), determined by $^1$H NMR spectroscopy. The thermodynamically unfavorable isomerization of DHAP was coupled to oxidation of the first-formed products GAP and *d*-GAP to give *h*-PGA and *d*-PGA, respectively, using GPDH. (A) The decrease with time in the fraction of remaining DHAP, calculated using eq 3. (B) The change with time in the fractional yields of the products of the enzymatic reaction of DHAP, normalized using the sum of the observed fractions of [1(*R*)-$^2$H]-DHAP, GAP (quantified as *h*-PGA) and [2(*R*)-$^2$H]-GAP (quantified as *d*-PGA), according to eqs 8−10. Short extrapolations of these data to zero time (solid lines) gave the initial product yields of the enzymatic reaction of DHAP, $f_E$, reported in Table 1. Key: (□) yield of *h*-PGA; (■) yield of *d*-PGA; (●) yield of [1(*R*)-$^2$H]-DHAP.

using the sum of the observed fractions of *d*-DHAP, *h*-PGA, and *d*-PGA according to eqs 8−10. The observed decrease

$$(f_{d-\mathrm{DHAP}})_E = \frac{f_{d-\mathrm{DHAP}}}{f_{d-\mathrm{DHAP}} + f_{h-\mathrm{PGA}} + f_{d-\mathrm{PGA}}} \quad (8)$$

$$(f_{h-\mathrm{PGA}})_E = \frac{f_{h-\mathrm{PGA}}}{f_{d-\mathrm{DHAP}} + f_{h-\mathrm{PGA}} + f_{d-\mathrm{PGA}}} \quad (9)$$

$$(f_{d-\mathrm{PGA}})_E = \frac{f_{d-\mathrm{PGA}}}{f_{d-\mathrm{DHAP}} + f_{h-\mathrm{PGA}} + f_{d-\mathrm{PGA}}} \quad (10)$$

in the fractional yield of *d*-DHAP (Figure 2B, ●) and increase in the fractional yield of *d*-PGA (Figure 2B, ■) with time is a result of TIM-catalyzed isomerization of *d*-DHAP to give *d*-GAP, which then undergoes irreversible oxidation to *d*-PGA.

Table 1 gives the initial fractional yields of the products of the TIM-catalyzed reactions of DHAP, $f_E$, determined by making a short extrapolation of the normalized product yields $(f_P)_E$ to zero reaction time (Figure 2B). This table presents data for the following experiments.

(1) The reaction of DHAP catalyzed by TIM from rabbit muscle in the presence of two different levels of GPDH from baker's yeast (entries 1 and 2).

(2) The reaction of DHAP in a control experiment in which authentic muscle TIM was omitted (entry 3). The slow isomerization and deuterium exchange reactions of DHAP observed in this experiment are presumably catalyzed by the

Table 1: Product Distributions for the Reaction of Dihydroxyacetone Phosphate Catalyzed by Triosephosphate Isomerase in $D_2O$ Buffered by 80 mM Imidazole at pD 7.9[a]

| | | amt (units/mL) | | | fractional yield of product[b] | | | |
|---|---|---|---|---|---|---|---|---|
| entry | TIM[c] (amt (units/mL)) | GPDH[d] | LDH[e] | | *h*-PGA[f] | *d*-PGA[f] | *d*-DHAP | methylglyoxal |
| 1 | rabbit (0.0059) | 0.3 | 1.3 | $f_T$[g] | 0.15 | 0.40 | 0.33 | 0.12 |
| | | | | $f_E$[h] | 0.17 | 0.45 | 0.38 | |
| 2 | rabbit (0.0017) | 0.6 | 1.4 | $f_T$[g] | 0.14 | 0.31 | 0.30 | 0.24 |
| | | | | $f_E$[h] | 0.19 | 0.41 | 0.40 | |
| 3 | none[i] | 0.6 | 1.4 | $f_T$[g] | 0.13 | 0.22 | 0.17 | 0.48 |
| | | | | $f_E$[h] | 0.25 | 0.42 | 0.33 | |
| 4 | chicken (0.0059) | 0.3 | 1.5 | $f_T$[g] | 0.15 | 0.37 | 0.35 | 0.14 |
| | | | | $f_E$[h] | 0.17 | 0.42 | 0.41 | |
| av | | | | $f_E$[j] | $0.18 \pm 0.01$ | $0.43 \pm 0.02$ | $0.40 \pm 0.02$ | |

$k_{ex}/(k_{C-2})_H = 4.56$;[k] $(k_{C-1})_D/(k_{C-2})_D = 0.93$[l]

[a] For reactions at 25 °C and $I = 0.15$ (NaCl) in the presence of 15 mM sodium hydrogenarsenate, 7 mM pyruvate, 0.1 mM NAD and various levels of GPDH and LDH. [b] Product yields were determined by $^1H$ NMR spectroscopy. [c] Activity for isomerization of DHAP (5 mM) in $H_2O$ at pH 7.5 and 25 °C. [d] Glyceraldehyde 3-phosphate dehydrogenase present to trap GAP and *d*-GAP to give the stable products *h*-PGA and *d*-PGA, respectively. [e] L-Lactic dehydrogenase present to catalyze regeneration of the NAD cofactor. [f] The thermodynamically unfavorable products GAP and *d*-GAP were rapidly and irreversibly oxidized by NAD to give *h*-PGA and *d*-PGA, respectively, in reactions catalyzed by GPDH. [g] Yields of the products of both the enzymatic and nonenzymatic reactions of DHAP, determined by extrapolation of the values of $f_P/(1 - f_{DHAP})$ to zero time, where $f_P$ is the observed fraction of the product (eqs 4−7) and $1 - f_{DHAP}$ is the fraction of DHAP that has undergone reaction. [h] Yields of the products of *only* the enzymatic reaction DHAP, determined by extrapolation of the normalized yields $(F_P)_E$ (eqs 8−10) to zero time (Figure 2B). [i] The slow turnover of DHAP in this experiment is catalyzed mainly by the low level of TIM present as a contaminant in the commercial preparation of yeast GPDH (see text). [j] Average value of $f_E$ for the reactions catalyzed by rabbit and chicken muscle TIM (entries 1, 2, and 4). [k] Rate constant ratio for partitioning of the TIM−enediol(ate) complex labeled with hydrogen at Glu-165 between hydron exchange with solvent $D_2O$ and intramolecular transfer of the substrate-derived hydrogen to product GAP. [l] Rate constant ratio for partitioning of the TIM−enediol(ate) complex labeled with deuterium at Glu-165 between deuterium transfer to C-1 to give *d*-DHAP and to C-2 to give *d*-GAP.

isomerase present as a contaminant in the commercial preparation of yeast GPDH and also by the lower level of TIM present as a contaminant in the commercial preparation of rabbit muscle LDH.

(3) The reaction of DHAP catalyzed by recombinant chicken muscle TIM (entry 4). In this experiment the preparations of both GPDH and LDH were freed of contaminating TIM activity by pretreatment with chloroacetol phosphate, an active-site-directed irreversible inhibitor of TIM (*24*).

## DISCUSSION

We have found that $^1H$ NMR spectroscopy is a powerful analytical method that can used to directly monitor the isomerization and isotope exchange reactions of (*R*)-glyceraldehyde (*25*), (*R*)-glyceraldehyde 3-phosphate (GAP, (*1*)), and dihydroxyacetone phosphate (DHAP, this work) catalyzed by triosephosphate isomerase in $D_2O$. Table 1 reports the product distributions, determined by $^1H$ NMR analysis, for the reaction of DHAP (5 mM) catalyzed by commercial rabbit muscle and recombinant chicken muscle TIM in $D_2O$, under conditions where the first-formed isomerization products GAP and [2(*R*)-$^2$H]-glyceraldehyde 3-phosphate (*d*-GAP) are rapidly and irreversibly converted to (*R*)-3-phosphoglycerate (*h*-PGA) and [2(*R*)-$^2$H]-3-phosphoglycerate (*d*-PGA), respectively (Scheme 3). These data show the following:

(1) *The initial products GAP and d-GAP are rapidly and quantitatively converted to h-PGA and d-PGA in reactions catalyzed by GPDH present in excess.* This is shown by the essentially identical (±10%) product distributions for the reactions catalyzed by rabbit muscle TIM in the presence of two different levels (50- or 350-fold excess) of the GPDH coupling enzyme (Table 1, entries 1 and 2). Note that the yield of methylglyoxal from the competing nonenzymatic elimination reaction of DHAP (*17*) increases as the concentration of added TIM is decreased.

(2) *The TIM present as a contaminant in the commercial preparation of yeast GPDH used as a coupling enzyme gives a product distribution very similar to that for TIM from rabbit muscle.* This was demonstrated in the control experiment conducted in the presence of only the coupling enzymes and no added authentic muscle TIM (Table 1, entry 3). The enediolate phosphate that is formed by the nonenzymatic deprotonation of DHAP in solution undergoes essentially exclusive elimination to form methylglyoxal (*17*). Therefore, the observed ca. 50% yield of the products of the isomerization and deuterium exchange reactions of DHAP in this experiment is very likely due to TIM present as a contaminant in the commercial preparation of yeast GPDH. The relative yields of the products *d*-DHAP, *h*-PGA, and *d*-PGA determined in this control experiment are similar to those determined for reactions in the presence of added rabbit and chicken muscle TIM.[2] This is consistent with the earlier conclusion that "the kinetic characteristics of the yeast enzyme [TIM] are very close to those of the chicken isomerase" *(15)*. This control experiment (Table 1, entry 3) also shows that the presence of small amounts of contaminating TIM in the coupling enzyme preparations does not have a significant effect on the observed product distribution for the reactions conducted in the presence of added authentic rabbit or chicken muscle TIM (Table 1, entries 1, 2, and 4).

[2] The error limits for the initial product yields determined for the slow reaction of DHAP in the absence of added authentic muscle TIM (Table 1, entry 3) are larger than for the other experiments in Table 1. However, these limits were not rigorously characterized and we are not certain that this difference is significant.

Scheme 4

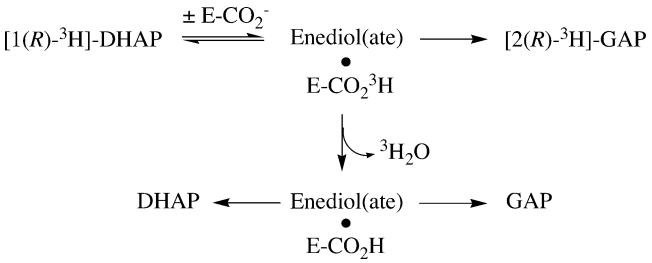


(3) *The same product distribution (±10%) is observed for the reactions of DHAP catalyzed by rabbit muscle and recombinant chicken muscle TIM in $D_2O$.* This is shown by entries 1 and 4. Note that the experiment with chicken muscle TIM employed coupling enzymes that were freed of TIM activity by pretreatment with chloroacetol phosphate.

*Direct Comparisons with Other Work.* The data in Table 1 show that 18% of the turnover of DHAP by muscle TIM in $D_2O$ occurs with intramolecular transfer of hydrogen to form GAP (quantified as its oxidation product *h*-PGA). The difference between the observations of 18% and 49% intramolecular transfer of hydrogen label from substrate to product in the TIM-catalyzed reactions of DHAP (this work) and GAP (*1*), respectively, in $D_2O$ is consistent with the 3-fold larger barrier to reaction of the enzyme-bound enediol(ate) intermediate to form GAP than for its reaction to form DHAP that was characterized by Knowles and co-workers (*3, 26*) (see below).

The specific radioactivity of the 3-phosphoglycerate formed in the coupled isomerization of [1(*R*)-$^3$H]-DHAP labeled with tracer tritium catalyzed by chicken muscle TIM in $H_2O$ increases from ca. 3% of the initial specific radioactivity of the substrate at ca. 50% conversion to product to 6% after complete reaction of [1(*R*)-$^3$H]-DHAP (*14*). The low specific radioactivity of the product formed during reaction of the first 50% of substrate reflects the discrimination isotope effect against reaction of the tritium-labeled substrate; this also results in a corresponding increase in the specific radioactivity of the remaining substrate during its reaction (*14*). The final specific radioactivity of the 3-phosphoglycerate product determined after complete reaction of [1(*R*)-$^3$H]-DHAP shows that 6% of the reaction occurs with intramolecular transfer of tritium to the first-formed product GAP (Scheme 4). Similarly, the reaction of [1(*R*)-$^2$H]-DHAP catalyzed by chicken muscle TIM in $H_2O$ has been reported to proceed with 6% intramolecular transfer of the deuterium label to give [2(*R*)-$^2$H]-GAP (*d*-GAP) (*27*).

The difference between the observations of 17% (Table 1, entry 4) and 6% (*14*) intramolecular transfer of the substrate-derived hydron to product during the chicken muscle TIM catalyzed reactions of DHAP in $D_2O$ and [1(*R*)-$^3$H]-DHAP in $H_2O$, respectively, appears to be larger than the experimental uncertainty in these results. Furthermore, results similar to those obtained in the first study of the isomerization of [1(*R*)-$^3$H]-DHAP catalyzed by chicken muscle TIM (*14*) have been reported in studies on TIM from yeast (*15, 16*) and on mutant forms of TIM from both chicken muscle (*28*) and yeast (*18*). Although we are unable to offer a full and unambiguous explanation, we suggest that the ca. 3-fold difference in the observed extent of intramolecular transfer of the hydron from substrate DHAP to product GAP determined in these two types of experiments is the result of a combination of several or all of the following smaller effects.

Scheme 5

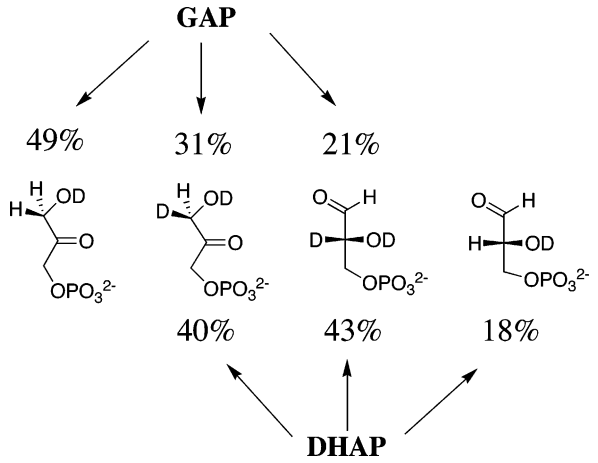


(1) A primary tritium isotope effect on hydron transfer to the enediol(ate) intermediate to form GAP. This isotope effect cannot be large, because there is only a 1.3-fold discrimination isotope effect against the formation of [2(*R*)-$^3$H]-GAP during the TIM-catalyzed isomerization of DHAP in tritiated water (*3, 29*).

(2) A relatively large extent of intramolecular transfer of the hydrogen label that is related to the higher initial concentration of DHAP used in this work (5 mM) as compared to that used in the earlier work (0.7−2.0 mM) (*14*). In experiments with TIM from yeast it has been shown that there is a triphasic ca. 2-fold variation in the fraction of intramolecular transfer of tritium from substrate [1(*R*)-$^3$H]-DHAP to product GAP as the initial concentration of DHAP is increased from 0.03 to 7.0 mM (*16*).

(3) A solvent deuterium isotope effect on partitioning of the TIM−enediol(ate) intermediate between hydron exchange with solvent and intramolecular transfer of the substrate-derived hydron to product.

(4) The cumulative effect of several small systematic or random experimental errors.

*Other Comparisons with Earlier Work.* Scheme 5 compares the product distributions for the reactions of GAP (*1*) and DHAP (this work) catalyzed by muscle TIM in $D_2O$. The product yields for the reaction of GAP give the apparent rate constant ratio $(k_{C-1})_H/k_{ex} = 0.49/0.51 = 0.96$ for partitioning of the TIM−enediol(ate) intermediate between protonation at C-1 and deuterium exchange with solvent (*1*), while the product yields for the reaction of DHAP give $(k_{C-2})_H/k_{ex} = 0.18/0.82 = 0.22$ for protonation at C-2 and deuterium exchange with solvent. With the assumption that $k_{ex}$ for exchange of the hydron bound to Glu-165 with solvent $D_2O$ is the *same* for the intermediate generated from the reactions of GAP and DHAP, then these partitioning ratios can be combined to give $(k_{C-1})_H/(k_{C-2})_H = 4.4$ for partitioning of the TIM−enediol(ate) intermediate between proton transfer to form $^1$H-labeled DHAP and GAP in $D_2O$ (Scheme 6). (Note, however, that the results discussed below suggest that this is, at best, an approximate assumption.)

A study of the TIM-catalyzed conversion of GAP to DHAP in tritiated water provided qualitative evidence that the rate constant for protonation of the reaction intermediate

Scheme 6

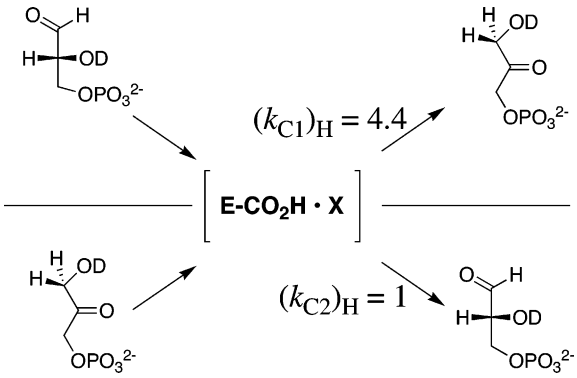


at C-1 to give DHAP is ca. 3-fold larger than that for protonation at C-2 to give GAP (*3*, *26*), which is in fair agreement with $(k_{C-1})_H/(k_{C-2})_H = 4.4$ observed here for reaction in $D_2O$.

The similar relative yields of *d*-GAP and *d*-DHAP formed during the TIM-catalyzed isomerization reactions of GAP and DHAP in $D_2O$ (Scheme 5) show that there are similar barriers to partitioning of the TIM−enediol(ate) between formation of the deuterium-labeled α-hydroxy aldehyde and ketone products. Therefore, we conclude that the change from hydrogen to deuterium at the protonated carboxylic acid side chain of Glu-165 in the TIM−enediol(ate) complex results in a decrease from $(k_{C-1})_H/(k_{C-2})_H \approx 4.4$ for partitioning of the hydrogen-labeled enzyme (Scheme 6) to $(k_{C-1})_D/(k_{C-2})_D \approx 1$ for partitioning of the deuterium-labeled enzyme. This is consistent with a large body of data from earlier work which shows that reaction of the TIM−enediol(ate) intermediate to form DHAP is limited by the isotopically sensitive proton-transfer step but that the formation of GAP from this intermediate is limited by the release of product from the enzyme (*3*, *26*, *29*, *30*). As a result, the change from E-$CO_2$H to E-$CO_2$D at the reaction intermediate will result in a decrease in $(k_{C-1})_L$ for formation of DHAP due to a primary deuterium isotope effect, little change in $(k_{C-2})_L$ for formation of GAP, and an overall decrease in the partitioning ratio $(k_{C-1})_L/(k_{C-2})_L$, as is observed in this work.

*Nature of the TIM−Enediol(ate) Intermediate.* The ratio of the yields of the deuterium-labeled products *d*-DHAP and *d*-GAP from the TIM-catalyzed isomerization of GAP in $D_2O$ gives a rate constant ratio $(k_{C-1})_D/(k_{C-2})_D = 1.48$ (*1*). This is significantly larger than $(k_{C-1})_D/(k_{C-2})_D = 0.93$ obtained from the yields of these products from the isomerization of DHAP in $D_2O$ (Scheme 5). The individual product yields can reproduced to better than ±10%, so that the resulting uncertainty in these ratios is no more than 20%, which is much smaller than the observed difference of ca. 50%. The observation of different product distributions from partitioning of the TIM−enediol(ate) intermediate generated from the enzyme-catalyzed deprotonation of GAP and DHAP in $D_2O$ provides evidence that the reaction of these two substrates does *not* proceed through a single, common, reaction intermediate.

The nonenzymatic base-catalyzed deprotonation of GAP in water gives the enediolate O-1 oxyanion, while the deprotonation of DHAP gives the O-2 oxyanion. However, in solution, the equilibration of these distinct intermediates by proton transfer between the electronegative oxygens is fast relative to proton transfer at carbon to form the α-hydroxy aldehyde or ketone (*17*). By comparison, the deprotonation of GAP bound to TIM gives an intermediate that is stabilized by an interaction with His-95 at O-1, while the deprotonation of DHAP gives an intermediate that is stabilized by an interaction with His-95 at O-2 (*18*−*20*). Our experimental results require that there is, at best, only partial equilibration of these two intermediates during the turnover of substrate to product, so that the relative steady-state concentrations of the two distinct intermediates labeled with deuterium at Glu-165 generated during the enzyme-catalyzed isomerization reactions of GAP and DHAP in $D_2O$ are different.

The *apparent* rate constant ratio for partitioning of the intermediate formed by the deprotonation of GAP and DHAP in tritiated water by H95Q mutant yeast TIM to give [1(*R*)-$^3$H]-DHAP and [2(*R*)-$^3$H]-GAP is infinity and zero, respectively (*18*). In other words, the reactions of *both* GAP and DHAP in tritiated water catalyzed by this mutant TIM result in transfer of tritium from solvent to product but *not* to unreacted substrate. This shows that removal of the imidazole side chain of His-95, which stabilizes the negative charge at O-1 or O-2 of the enediolate intermediate for the wild type enzyme (*18*−*20*), results in a dramatic difference in the partitioning of the two intermediates generated by the deprotonation of GAP and DHAP.

Scheme 7 shows mechanisms that were proposed to rationalize the observed product distributions for the reactions of DHAP and GAP catalyzed by H95Q mutant yeast TIM in tritiated water (*18*). Deprotonation of DHAP (Scheme 7A) and of GAP (Scheme 7B) gives the enediolate O-2 and O-1 oxyanions, respectively. The H95Q mutation eliminates the hydrogen bond that is proposed to stabilize these oxyanions (*18*−*20*) and is therefore expected to result in an increase in the basicity of these enolate oxygens. This is proposed to promote tritium exchange through transfer of the substrate-derived proton from the side chain of Glu-165 to the enediolate oxyanion, followed by reprotonation of this side chain by the second, tritium-labeled, enediol hydroxyl. This

Scheme 7

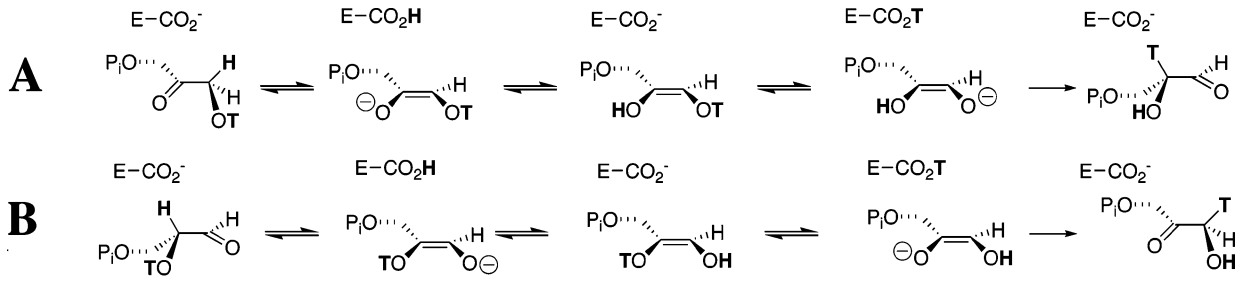

sequence of reactions tightly *couples* hydron exchange at the side chain of Glu-165 to conversion of the "substrate-derived" enediolate intermediate to the "product-forming" enediolate. This will lead to transfer of tritium from solvent to product, but not to remaining substrate, provided protonation of the enediolate intermediate at carbon to form product is faster than the steps leading to the formation of tritium-labeled substrate. It is important to note that tritium-labeled substrate *cannot be formed* by the microscopic reverse of the steps shown in parts A and B of Scheme 7. Rather, this reaction must follow a different pathway for proton transfer between the two oxygens of the enediolate.

Our results show that wild type muscle TIM in a solvent of $D_2O$ catalyzes the incorporation of deuterium from solvent into product faster than the incorporation of deuterium into the substrate when the substrate is *either* DHAP *or* GAP (Scheme 5). Therefore, the wildtype and H95Q mutant TIMs are similar in that each catalyzes the preferential transfer of label from solvent to product, but they differ in that only the wildtype enzyme catalyzes the slower, competing, transfer of label into the remaining substrate. This suggests that the mechanistic features of the H95Q mutant enzyme that result in preferential transfer of label from solvent to product are partly preserved for the wild type enzyme and that one role of His-95 is to promote proton transfer between O-1 and O-2 of the enediolate by a pathway that does not involve Glu-165. For example, this proton transfer at the wild type enzyme might occur by protonation of an enediolate oxygen by His-95 to form the enediol hydrogen bonded to an imidazolate anion, followed by deprotonation of the second oxygen to regenerate a neutral imidazole and a second enediolate intermediate.

*Summary.* The analytical methods we have developed to monitor the fate of the acidic hydrogen at GAP or DHAP during the turnover of these substrates by rabbit and chicken muscle TIM in $D_2O$ are simpler and more direct than related experiments that monitor the fate of a tritium label at the substrate for reactions in $H_2O$ (*3*, *14*). The product distributions for the enzyme-catalyzed reactions of the hydrogen-labeled substrates GAP and DHAP in $D_2O$ can be monitored directly by $^1H$ NMR spectroscopy. By comparison, experiments which employ a tritium label may require the synthesis of tritium-labeled substrates, and they always require the purification of each tritium-labeled compound prior to the determination of its specific radioactivity.

There is good overall agreement between the results reported here and the classic studies of Knowles and co-workers (*3*, *14*, *26*, *27*, *29*−*33*), with one significant difference and one new observation. The difference is that significantly higher levels of intramolecular transfer of hydrogen label from substrate to product are observed for the TIM-catalyzed reactions of both GAP and DHAP in $D_2O$ than for the reaction of [1(*R*)-$^3$H]-DHAP in $H_2O$. This shows that, for reactions in $D_2O$, the substrate-derived hydron at the carboxylic acid side chain of Glu-165 and those of bulk solvent cannot be "essentially at equilibrium" in the TIM−enediol(ate) complex, which stands in sharp contrast with the conclusion drawn in the earlier work (*3*).

The new observation from this work is that the relative yields of the deuterium-labeled α−hydroxy aldehyde and ketone products that form by partitioning of the intermediates generated by TIM-catalyzed deprotonation of DHAP and GAP in $D_2O$ are different. This result is not unexpected for a reaction that occurs within the restricted confines of an enzyme active site. It is consistent with the notion, discussed in greater detail in the preceding paper (*1*), that the enzyme-bound enediol(ate) intermediate is largely sequestered from the bulk solvent.

## REFERENCES


1. O'Donoghue, A. C., Amyes, T. L., and Richard, J. P. (2005) Hydron Transfer Catalyzed by Triosephosphate Isomerase. The Products of Isomerization of (*R*)-Glyceraldehyde 3-Phosphate in $D_2O$, *Biochemistry* **44**, 2610−2621.
2. Rieder, S. V., and Rose, I. A. (1959) Mechanism of the Triose Phosphate Isomerase Reaction, *J. Biol. Chem. 234*, 1007−1010.
3. Knowles, J. R., and Albery, W. J. (1977) Perfection in Enzyme Catalysis: The Energetics of triosephosphate Isomerase, *Acc. Chem. Res. 10*, 105−111.
4. Amyes, T. L., and Richard, J. P. (1992) Generation and Stability of a Simple Thiol Ester Enolate in Aqueous Solution, *J. Am. Chem. Soc. 114*, 10297−10302.
5. Amyes, T. L., and Richard, J. P. (1996) Determination of the p$K_a$ of Ethyl Acetate: Brønsted Correlation for Deprotonation of a Simple Oxygen Ester in Aqueous Solution, *J. Am. Chem. Soc. 118*, 3129−3141.
6. Richard, J. P., Williams, G., and Gao, J. (1999) Experimental and Computational Determination of the Effect of the Cyano Group on Carbon Acidity in Water, *J. Am. Chem. Soc. 121*, 715−726.
7. Richard, J. P., and Nagorski, R. W. (1999) Mechanistic Imperatives for Catalysis of Aldol Addition Reactions: Partitioning of the Enolate Intermediate between Reaction with Brønsted Acids and the Carbonyl Group, *J. Am. Chem. Soc. 121*, 4763−4770.
8. Rios, A., Amyes, T. L., and Richard, J. P. (2000) Formation and Stability of Organic Zwitterions in Aqueous Solution: Enolates of the Amino Acid Glycine and Its Derivatives, *J. Am. Chem. Soc. 122*, 9373−9385.
9. Nagorski, R. W., and Richard, J. P. (2001) Mechanistic Imperatives for Aldose-Ketose Isomerization in Water: Specific, General Base- and Metal Ion-Catalyzed Isomerization of Glyceraldehyde with Proton and Hydride Transfer, *J. Am. Chem. Soc. 123*, 794−802.
10. Rios, A., Richard, J. P., and Amyes, T. L. (2002) Formation and Stability of Peptide Enolates in Aqueous Solution, *J. Am. Chem. Soc. 124*, 8251−8259.
11. Chiang, Y., Griesbeck, A. G., Heckroth, H., Hellrung, B., Kresge, A. J., Meng, Q., O'Donoghue, A. C., Richard, J. P., and J. Wirz. (2001) Keto−Enol/Enolate Equilibria in the *N*-Acetylamino-*p*-methylacetophenone System. Effect of a *β*-Nitrogen Substituent, *J. Am. Chem. Soc. 124*, 8979−8984.
12. Richard, J. P., Williams, G., O'Donoghue, A. C., and Amyes, T. L. (2002) Formation and Stability of Enolates of Acetamide and Acetate Anion: An Eigen Plot for Proton Transfer at α-Carbonyl Carbon, *J. Am. Chem. Soc. 124*, 2957−2968.
13. Crugeiras, J., and Richard, J. P. (2004) A Comparison of the Electrophilic Reactivities of $Zn^{2+}$ and Acetic Acid as Catalysts of Enolization: Imperatives for Enzymatic Catalysis of Proton Transfer at Carbon, *J. Am. Chem. Soc. 126*, 5164−5173.
14. Herlihy, J. M., Maister, S. G., Albery, W. J., and Knowles, J. R. (1976) Energetics of Triosephosphate Isomerase: The Fate of the 1(*R*)-$^3$H Label of Tritiated Dihydroxyacetone Phosphate in the Isomerase Reaction, *Biochemistry 15*, 5601−5607.
15. Nickbarg, E. B., and Knowles, J. R. (1988) Triosephosphate Isomerase: Energetics of the Reaction Catalyzed by the Yeast Enzyme Expressed in *Escherichia coli*, *Biochemistry 27*, 5939−5947.
16. Harris, T. K., Cole, R. N., Comer, F. I., and Mildvan, A. S. (1998) Proton Transfer in the Mechanism of Triosephosphate Isomerase, *Biochemistry 37*, 16828−16838.
17. Richard, J. P. (1984) Acid−Base Catalysis of the Elimination and Isomerization Reactions of Triose Phosphates, *J. Am. Chem. Soc. 106*, 4926−4936.
18. Nickbarg, E. B., Davenport, R. C., Petsko, G. A., and Knowles, J. R. (1988) Triosephosphate Isomerase: Removal of a Putatively Electrophilic Histidine Residue Results in a Subtle Change in Catalytic Mechanism, *Biochemistry 27*, 5948−5960.

19. Komives, E. A., Chang, L. C., Lolis, E., Tilton, R. F., Petsko, G. A., and Knowles, J. R. (1991) Electrophilic Catalysis in Triosephosphate Isomerase: The Role of Histidine-95, *Biochemistry 30*, 3011−3019.
20. Lodi, P. J., and Knowles, J. R. (1991) Neutral Imidazole Is the Electrophile in the Reaction Catalyzed by Triosephosphate Isomerase: Structural Origins and Catalytic Implications, *Biochemistry 30*, 6948−6956.
21. Plaut, B., and Knowles, J. R. (1972) pH-Dependence of the triose phosphate isomerase reaction, *Biochem. J. 129*, 311−320.
22. Veech, R. L., Raijman, L., Dalziel, K., and Krebs, H. A. (1969) Disequilibrium in the triose phosphate isomerase system in rat liver, *Biochem. J. 115*, 837−842.
23. Rose, I. A., O'Connell, E. L., and Mehler, A. H. (1965) Mechanism of the aldolase reaction, *J. Biol. Chem. 240*, 1758−1765.
24. Hartman, F. C. (1970) Isolation and Characterization of an Active-Site Peptide from Triose Phosphate Isomerase, *J. Am. Chem. Soc. 92*, 2170−2172.
25. Amyes, T. L., O'Donoghue, A. C., and Richard, J. P. (2001) Contribution of Phosphate Intrinsic Binding Energy to the Rate Acceleration of Triosephosphate Isomerase, *J. Am. Chem. Soc. 123*, 11325−11326.
26. Fletcher, S. J., Herlihy, J. M., Albery, W. J., and Knowles, J. R. (1976) Energetics of Triosephosphate Isomerase: The Appearance of Solvent Tritium in substrate Glyceraldehyde 3-Phosphate and in Product, *Biochemistry 15*, 5612−5617.
27. Fisher, L. M., Albery, W. J., and Knowles, J. R. (1976) Energetics of Triosephosphate Isomerase: The Nature of the Proton Transfer between the Catalytic Base and Solvent Water, *Biochemistry 15*, 5621−5626.
28. Raines, R. T., Sutton, E. L., Straus, D. R., Gilbert, W., and Knowles, J. R. (1986) Reaction Energetics of a Mutant Triose Phosphate Isomerase in Which the Active-Site Glutamate Has Been Changed to Aspartate, *Biochemistry 25*, 7142−7154.
29. Maister, S. G., Pett, C. P., Albery, W. J., and Knowles, J. R. (1976) Energetics of TriosephosphateIsomerase: The Appearance of Solvent Tritium in Substrate Dihydroxyacetone Phosphate and in Product, *Biochemistry 15*, 5607−5612.
30. Leadlay, P. F., Albery, W. J., and Knowles, J. R. (1976) Energetics of Triosephosphate Isomerase: Deuterium Isotope Effects in the Enzyme-Catalyzed Reaction, *Biochemistry 15*, 5617−5620.
31. Albery, W. J., and Knowles, J. R. (1976) Deuterium and Tritium Exchange in Enzyme Kinetics, *Biochemistry 15*, 5588−5600.
32. Albery, W. J., and Knowles, J. R. (1976) Free-Energy Profile for the Reaction Catalyzed by Triosephosphate Isomerase, *Biochemistry 15*, 5627−5631.
33. Albery, W. J., and Knowles, J. R. (1976) Evolution of Enzyme Function and the Development of Catalytic Efficiency, *Biochemistry 15*, 5631−5640.

BI047953K